We are IntechOpen, the world's leading publisher of Open Access books Built by scientists, for scientists

6,900
Open access books available

185,000
International authors and editors

200M
Downloads

Our authors are among the

154
Countries delivered to

TOP 1%
most cited scientists

12.2%
Contributors from top 500 universities



WEB OF SCIENCE™

Selection of our books indexed in the Book Citation Index in Web of Science™ Core Collection (BKCI)

Interested in publishing with us?
Contact book.department@intechopen.com

Numbers displayed above are based on latest data collected.
For more information visit www.intechopen.com



Chapter 10

Cr(VI) Adsorption Onto Biomass Waste Material-Derived Activated Carbon

Dilek Duranoğlu and Ulker Beker

Additional information is available at the end of the chapter

http://dx.doi.org/10.5772/60206

Abstract

Activated carbons derived from biomass waste material can be favorable compared to conventional activated carbons with respect to their adsorptive properties, low cost, and renewable sources. Literature about Cr(VI) adsorption onto biomass waste material based activated carbons has been reviewed. Activated carbon derived from peach stone was used for Cr(VI) adsorption from aqueous media. The effects of process parameters like pH, temperature, concentration, and adsorbent amount on Cr(VI) removal were examined with aspect of equilibrium and kinetics.

Peach stone based activated carbon showed high Cr(VI) adsorption capacity. Cr(VI) adsorption was strongly pH-dependent and superior at low pH. Freundlich model well expressed Cr(VI) adsorption. Adsorption kinetics followed the pseudo second-order kinetic model which consists of chemisorption. Possible adsorption mechanism was suggested in three steps: (i) Cr(VI) adsorption onto positively charged groups, (ii) reduction to Cr(III), (iii) adsorption of Cr(III) while a little amount of it releases to the aqueous phase.

Keywords: Cr(VI), activated carbon, biomass, peach stone, adsorption

1. Introduction

Water pollution by chromium is due to both natural and anthropogenic sources like leather, textile, steel producing, magnetic tapes, wood protection, paper, chemical manufacturing, metal plating, battery, and pigment industries. According to the EPA (2000) [1], chromium is

INTECH
open science | open minds

© 2015 The Author(s). Licensee InTech. This chapter is distributed under the terms of the Creative Commons Attribution License (http://creativecommons.org/licenses/by/3.0), which permits unrestricted use, distribution, and reproduction in any medium, provided the original work is properly cited.

the second common metal which exists in contaminated fields. It exists in different oxidation states ranging from –2 to +6. However, the most frequently encountered chromium species are trivalent and hexavalent forms since the +2, +4, and +5 forms are unstable and are easily converted to trivalent form.

Cr(III), which is the most thermodynamically stable chromium form, is relatively innocuous due to the poor biological cell permeability and is an essential trace element for living organisms. According to Eh–pH diagram (Figure 1), chromium hydroxyl species exist as $CrOH^{2+}$, $Cr(OH)_2^+$, $Cr(OH)_3$, and $Cr(OH)_4^-$ at pH > 3.5 while Cr(III) predominates at pH < 3.0. The second stable chromium form, Cr(VI), is generally produced by anthropogenic activities. Cr(VI) is a strong oxidant and reacts readily with any oxidizable organic material, hence converts to trivalent form. In the absence of organic matter, especially under aerobic conditions, it can be stable for long time [2]. It exists primarily as salts of chromic acid (H_2CrO_4), hydrogen chromate ion ($HCrO_4^-$), and chromate ion (CrO_4^{2-}), depending on pH (Figure 2). Predominant Cr(VI) species in the solution is $HCrO_4^-$ at pH between 1.0 and 6.5 while CrO_4^{2-} ions are dominant above pH 6.5 [3]. Dichromate anions ($Cr_2O_7^{2-}$) can be found only at high concentrations about more than 1 g/L.

Chromium is considered the fourteenth most noxious heavy metal [4]. Cr(VI) compounds are more toxic and carcinogenic even at low concentrations and over a wide range of pH values. High concentrations of Cr(VI) cause water quality problem in natural water sources, and health problem included lung cancer as well as kidney, liver, and gastric damage [5, 6] for human. Contact with chromium can also cause skin irritation [7]. Because of its toxicity and carcinogenic nature, Cr(VI) compounds must be removed before discharging to the environment. The permissible limit of Cr(VI) for discharge into inland surface water is 0.1 mg/L [8, 9]. However, American Environmental Protection Agency (EPA) limits Cr(VI) concentration in potable water as 0.05 mg/L [1].

The most common methods of Cr(VI) removal from aqueous system are chemical precipitation, ion exchange, membrane processes, electrodialysis, and adsorption [7, 10–13]. Among them, chemical precipitation is the most commonly used method. However, chemical precipitation yields large quantities of sludge, which is difficult to dispose directly or treat further. Moreover, chemical precipitation method is not applicable for low concentrations.

However, adsorption by activated carbon is considered to be an effective process for chromium removal due to high specific surface area, pore volume, and specific surface functionalities of activated carbon; application in this field is not common. The limited selectivity and high cost are the main obstacles for using commercial activated carbon in order to remove chromium species from aqueous media. Many researchers have studied on chromium adsorption onto activated carbon during the past ten years. A significant amount of them have used several biomass waste materials as activated carbon source. Activated carbons derived from biomass waste material can be favorable compared to conventional activated carbons with respect to their adsorptive properties, low cost, and renewable sources; in addition, evaluation of this biomass waste materials as activated carbon precursor prevents solid waste pollution problem.

http://dx.doi.org/10.5772/60206

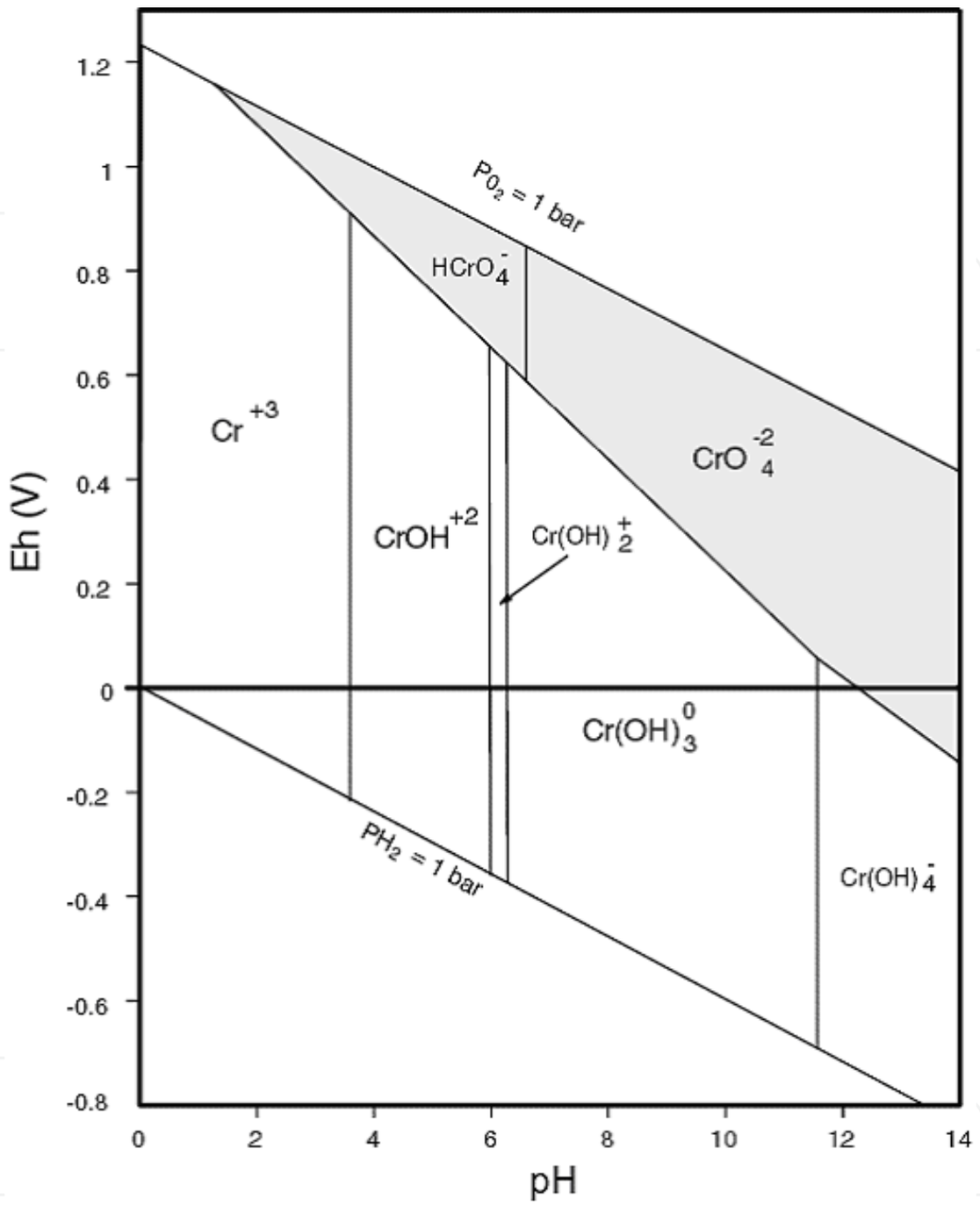


Figure 1. Eh–pH diagram for chromium [1]

In this chapter, the studies about Cr(VI) adsorption onto biomass based activated carbons have been reviewed and Cr(VI) adsorption onto activated carbon derived from peach stone has been studied. The effects of process parameters like pH, temperature, concentration, and adsorbent amount on chromium removal have been examined. Experimental results have been discussed in aspect of equilibrium and kinetics. In addition, possible chromium adsorption mechanisms have been discussed.

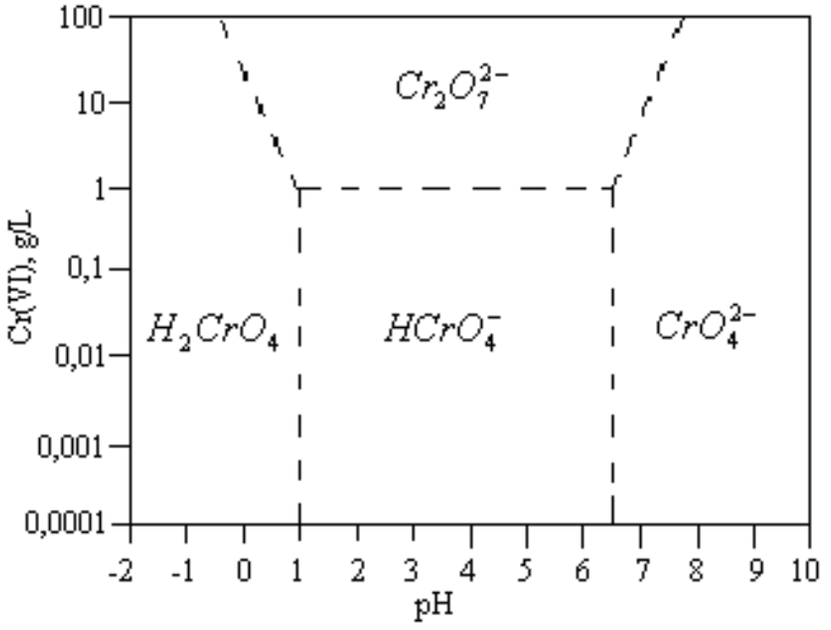


Figure 2. Speciation diagram of Cr(VI) [3]

2. Cr(VI) adsorption onto biomass-derived activated carbons

Activated carbons derived from wood, coal, and coconut shells are only available on the market although the activated carbons derived from biomass waste materials can be favorable with respect to their adsorptive properties, low cost, and renewable sources. The biomass waste materials are usually used as an energy source, burned in the field or spilled into the environment in a noncontrolled way. Evaluation of biomass waste materials as activated carbon precursors also aids to prevent solid waste pollution problem. The availability and the abundance of biomass waste material are two critical points in order to decide which biomass waste material will be used. Various biomass waste materials have been used to develop low cost activated carbons that have relatively high adsorption capacity.

Groundnut was treated with concentrated H_2SO_4 which is then carbonized at 150–155°C during 24 h (GNH) [14]. A part of produced carbon was impregnated with silver nitrate (SIGNH). Cr(VI) adsorption capacity of both SIGNH and GNH were 11.4 and 7.0 mg/g, respectively. Maximum Cr(VI) adsorption was at pH 3. Freundlich model represented the experimental data for both samples.

Researchers produced steam activated carbon from olive bagasse in reference [15] in order to remove Cr(VI) from aqueous solution. Produced microporous activated carbon had 718 m^2/g of BET surface area and 0.3699 cm^3/g of total pore volume. Cr(VI) adsorption capacity of activated carbon was dependent upon pH and maximum removal was obtained at pH 2 with 48.5 mg/g Cr(VI) adsorption capacity. High adsorption capacity at low pH was explained with neutralizing negatively charged adsorbent surface, thereby reducing the hindrance to the diffusion of chromate ions. In addition, the authors reported that Cr(VI) could be reduced to

http://dx.doi.org/10.5772/60206

trivalent form at highly acidic medium in the presence of activated carbon, but there was no reduction in their case. They only proved this with the pH increment from 2 to 4 during the experiment, and Cr(III) do not precipitate at this pH. On the other hand, one should keep in mind that Cr(III) can adsorb by carbon surface which oxidized as a result of reduction reaction, and oxidized carbon surface is more attractive for Cr(III) cations than the previous [16]. In order to verify this, Cr(III) concentration in the solution and in the solid phase should be determined. Equilibrium time for Cr(VI) removal was 10 h [15]. Adsorption of Cr(VI) on the olive bagasse based activated carbon followed pseudo second-order kinetic model. Langmuir model fitted better than the other models (Freundlich, Dubinin–Radushkevich (D–R), Temkin and Frumkin equations). Adsorption is chemical in nature and the process is endothermic ($\Delta H° = 39.45$ kJ/mol). Adsorption energy was in the range of 18.99–21.11 kJ/mol, which is bigger than the physical adsorption. Overall, it can be concluded from the results of thermodynamics and energy calculations that main mechanisms of Cr(VI) adsorption onto olive bagasse based activated carbon are chemisorption or reduction coupled adsorption.

Researchers used almond shell based activated carbon, which was activated with H_2SO_4 at 200°C during 24 h, for Cr(VI) adsorption [17]. The activated carbon has 412 m^2/g BET surface area and pH_{PZC} of carbon is 5.26. Cr(VI) adsorption was favored at pH 1 at 293 K with 144 mg/g capacity value. The authors explained the high adsorption capacity at low pH with the electrostatic attraction between the positively charged groups of carbon surface and $HCrO_4^-$ anions. Experimental data fitted the Freundlich model well. Thermodynamic studies indicated the spontaneous nature of the adsorption process was endothermic. The rise of adsorption with temperature was interpreted with enlarging the pore size to some extent by the authors.

Date palm seed was treated with concentrated H_2SO_4 for 5 h, then boiled for 20 h in a fume hood [18]. Maximum adsorption was noticed at pH 2 due to the electrostatic attraction between the positively charged groups of carbon surface and $HCrO_4^-$ anions. Various theoretical adsorption models (Langmuir, Freundlich, Temkin, Redlich–Peterson, Koble–Corrigan, and Dubinin–Radushkevich) were applied and all models represented the data reasonably well except Dubinin–Radushkevich equation. Adsorption equilibrium time was 180 min. Kinetic data obeyed the pseudo first-order kinetic model. Moreover, Elovich kinetic model had also very high correlation coefficient values.

Oil palm fiber was treated with concentrated H_2SO_4 at 150°C for 24 h in a muffle furnace [19]. Treated oil palm fiber was used for Cr(VI) removal. Maximum Cr(VI) adsorption capacity was 40 mg/g at 200 mg/L of initial Cr(VI) concentration, 5 g/L of adsorbent dosage, pH 1.5, and 28°C of temperature. Cr(VI) removal sharply reduced when the initial pH of the solution was increased to higher values. The authors explained this as same in reference [15] that low pH causes neutralizing of adsorbent surface charge by H^+ ions in the solution, hence Cr(VI) anions can diffuse to the surface easily. Equilibrium time was 6 h and Cr(VI) adsorption kinetics represented well by pseudo second-order kinetic model. The authors interpreted this compliance with chemical adsorption or chemisorption between the adsorbent and the adsorbate. Although Cr(VI) adsorption could be represented by both Freundlich ($R^2 = 0.8775$) and Langmuir ($R^2 = 0.8715$) isotherms, the Freundlich model showed better fit to the experimental

isotherm data. The authors also reported that desorption of Cr(VI) from treated palm fiber was very difficult.

Sugarcane husk and eucalyptus wood were pyrolized at 700°C for 2 h, then the char carbonized at 900°C under CO_2 flow during 4 h after treating with HNO_3 in reference [20]. For chemical activation, sugarcane husk and eucalyptus wood were activated at 900°C under nitrogen for 2 h after impregnation with H_3PO_4. The produced activated carbons have 260–367 m^2/g BET surface area and 0.865–1.234 cm^3/g total pore volume. Activated carbons have higher acidic groups and pore volume comparing to the literature. Comparing sugarcane husk and eucalyptus wood for Cr(VI) adsorption, sugarcane husk based one was more effective than the other for both physical and chemical treatment. Activated carbons obtained by the chemical method show a higher Cr(VI) adsorption capacity and the highest capacity (28 mg/g) was obtained at pH = 5 with chemically activated sugarcane husk based carbon.

Activated carbon was prepared from tamarind wood with zinc chloride in order to adsorb Cr(VI) from aqueous solution [21]. Micro porous activated carbon was obtained with 1322 m^2/g BET surface area and 1.042 cm^3/g pore volume. The authors observed that Cr(VI) adsorption percent decreased with pH in the range of pH 1–6. After pH 6.5, no more adsorption took place at all. Maximum adsorption capacity of about 28 mg/g was obtained at pH 1. It is very well known that pH is the most important parameter which affects both adsorbent and adsorbate ionic state. Researchers reported the adsorption mechanism with electrostatic attraction between negatively charged chromate/dichromate species and positively charged surface functional groups on the carbon surface at acidic media [21]. Adsorption rate was reduced above pH 3.0. According to the authors, physical adsorption has taken an important role, and exchange mechanism might have reduced after pH 3.0. The pseudo second-order kinetic model fitted the data better than pseudo first-order kinetic model. Webber Morris and Boyd kinetic models have been applied and it was found that the film diffusion is the rate control step for chromium adsorption. The Cr(VI) adsorption isotherm followed both linearized Freundlich and Langmuir model. Cr(VI) adsorption onto activated carbon produced was endothermic in nature. However, there was no explanation about the magnitude of adsorption enthalpy (ΔH° = 34.54–53.53 kJ/mol).

Researchers carbonized rice husk and saw dust at 150°C in hot air oven after treated with H_2SO_4 in [22]. The specific surface area of the produced RHC was 1.12 m^2/g and SDC was 1.16 m^2/g. Cr(VI) adsorption was favored at pH 2 and the maximum adsorption capacity was found as 47.8 mg/g and 53.1 mg/g at 250 mg/L initial Cr(VI) and 4 g/L adsorbent concentration for RHC and SDC, respectively. Similar to the others, the authors interpreted the pH effect with the electrostatic attraction between the highly protonated carbon surface and the $HCrO_4^-$ anions. The authors reported that Langmuir, D–R models, and Temkin isotherm fitted experimental data well. However, when looking at the linearized plots of both models, only Langmuir and Freundlich model showed the straight line with the experimental data. Adsorption energy values were calculated by using D–R model as lesser than 8 kJ/mol, which indicated the physical adsorption. As a result of dynamic investigation, it was obtained that Cr(VI) adsorption onto RHC and SDC has increased with time and remained constant after 120 min. Adsorption kinetics followed the pseudo second-order kinetic model very well

http://dx.doi.org/10.5772/60206

according to the correlation coefficients and the differences between the calculated and experimental adsorption capacities. The authors desorbed 55.48% and 53.03% of Cr(VI) by KI solution and 65.04% and 68.84% by HCl solution from RHC and SDC, respectively.

Activated carbon was prepared by burning the rice straw in the air in order to use as an adsorbent for Cr(VI) removal [23]. Cr(VI) was completely removed from solution in 12 h at pH 1 and the removal capacity was 20 mg/g, increasing pH resulted in decreasing the removal rate and capacity. Cr(III) was detected in the solution and as bounded to the carbon surface at pH 1–3. XPS results showed that Cr bound to carbon at any studied pH (pH 1–5) was predominately in its trivalent form. According to their mechanism, Cr(VI) anions first adsorbed on the carbon surface and adsorbed Cr(VI) reduced to Cr(III), consequently. The Cr(III) ions are either in the solution or bound to carbon surface.

Researchers in reference [24] prepared activated carbon (THAC) from Trapa natans husk, water chestnut, by using H_3PO_4 impregnation. In addition, Fe was loaded onto activated carbon (THAC-Fe). BET surface area and pore volume of THAC and THAC-Fe adsorbents were 782.86 m^2/g, 920.13 m^2/g, and 0.498 cm^3/g, 0.618 cm^3/g, respectively. pH_{PZC} values were 6.20 and 3.77 for THAC and THAC-Fe, respectively. Both produced sorbents were used for Cr(VI) adsorption from aqueous solution. Cr(VI) removal efficiency decreased dramatically from 100% to 2.1% as the initial solution pH increased from 3 to 11. The authors explained this with the electrostatic attraction between protonated carbon surface at $pH < pH_{PZC}$ and Cr(VI) anions as same as the most workers. It was reported that iron significantly enhanced the Cr(VI) adsorption capacity of the activated carbon. This was explained with larger surface area and pore volume, more acidic functional groups of THAC-Fe. Furthermore, the iron oxides have high affinity and selectivity toward Cr(VI) oxyanions. Pseudo second-order model well represented the kinetic data. It was noticed that both external mass transfer and intra-particle diffusion controlled the Cr(VI) adsorption rate. Tempkin and Freundlich models gave the best correlations for experimental equilibrium data. The maximum adsorption capacity was 11.83 mg/g. The authors interpreted the positive value of $\Delta H°$ with the endothermic nature of the adsorption. However, there was no explanation about the magnitude of adsorption enthalpy ($\Delta H° = 70.844$ kJ/mol). Very little desorption of Cr(VI) was interpreted with chemisorption.

Syzygium jambolanum nut, an agricultural waste, was chemically activated with ammonium per sulfate in the presence of sulphuric acid at 140–160°C and then subjected to thermal activation at 800–850°C in CO_2 atmosphere [25]. BET surface area and bulk density of produced activated carbon was 660 m^2/g and 0.63 g/mL, respectively. Maximum Cr(VI) removal was obtained at pH 2. High Cr(VI) removal in highly acidic media was interpreted with the electrostatic attraction of Cr(VI) in the anionic form and protonated adsorbent surface. Kinetic studies indicated that 4-hour-equilibration time was sufficient for maximum Cr(VI) removal and the removal process followed pseudo second-order kinetic model. It was also noticed that the film diffusion process was the rate-determining step. Freundlich adsorption model better represented the experimental data than Langmuir and Tempkin models. Eighty-five percent of Cr(VI) was eluted with 10% H_2O_2 and 1 M NaOH. Negative $\Delta G°$ value commented the feasibility and the spontaneous nature of the adsorption process.

Palm shell based steam activated carbon was modified with polyethyleneimine in [26]. Maximum 20 mg/g of Cr(VI) adsorption capacity was obtained with polyethyleneimine impregnated palm shell based activated carbon at 200 mg/L of initial concentration and pH 3–4. It was informed that adsorption capacity increased with pH up to pH 4, then it reduced by further pH increment. The adsorption took place between the anionic Cr(VI) species and polyethyleneimine, which is protonated at pH < 10. Cr(VI) adsorption was interpreted with the interaction between the Cr(VI) species and the protonated amine groups of polyethyleneimine. Freundlich model described the Cr(VI) adsorption onto modified activated carbon very well.

Algae bloom residue was converted to activated carbon by applying H_3PO_4 impregnation at 400°C [27]. The Cr(VI) adsorption capacity was superior at pH 1 due to the electrostatic attraction between protonated surface functional groups on carbon and negatively charged chromium species. Adsorption capacity was sharply declined by increasing pH since the deprotonation of surface functional groups. Maximum Cr(VI) adsorption capacity was 155.52 mg/g at 200 mg/L initial concentration, at pH 1. Both Langmuir and Freundlich models represented the data with high correlation coefficient (R^2 =0.991, 0.994, respectively), indicating both monolayer and heterogeneous surface conditions may exist. The authors indicated the physical adsorption is the major process since calculated mean free adsorption energy was 3.28 kJ/mol, which was lesser than 16 kJ/mol. Tempkin constant related to the heat of Cr(VI) adsorption onto activated carbon was estimated at 18.58 kJ/mol, indicating weak interaction between Cr(VI) ions and the carbon surface. Kinetic studies showed that 300 min of equilibration time was sufficient for maximum Cr(VI) removal and the removal process followed both pseudo first-order and pseudo second-order kinetic models according to the high correlation coefficients. However, the pseudo second-order model fits better the experimental data. Overall, the authors informed that there was more than one mechanism involved in the actual process.

Sugarcane bagasse-derived activated carbon was developed with chemical $ZnCl_2$ activation [28]. Central composite design method was applied to optimize the experimental conditions like adsorbent dosage, initial Cr(VI) concentration, temperature, and pH. Maximum Cr(VI) adsorption capacity was about 9.8 mg/g (87.01 %) at optimum conditions like 40°C, 77.5mg/L initial Cr(VI) concentration and pH 8.58. Converse to the similar works, the authors found high pH for optimum Cr(VI) removal with produced activated carbon. The authors did not give any explanation about this situation.

Highly microporous activated carbon was developed (S_{BET}: 1462 m^2/g V_{tot}: 0.638 cm^3/g) from apricot stone by using H_3PO_4 impregnation at 400°C [29]. The produced activated carbon was used for Cr(VI) adsorption from aqueous solution in batch system. Box-Behnken design method was used to optimize the process parameters. The maximum Cr(VI) adsorption capacity (234.28 mg/g) was found at pH 2 and the capacity decreased with increasing pH. The authors explained high adsorption capacity at low pH with the electrostatic attraction between the protonated carboxyl groups on carbon surface and the negatively charged hydrogen chromate ions. The carboxyl groups are protonated (AC-$COOH_2^+$) at low pH. Consecutive formation of neutral (AC$(COOH)^0$) and ionized (AC-COO^-) form with the rising pH leads to

http://dx.doi.org/10.5772/60206

a decreased electrostatic attraction between these groups and anionic Cr(VI) species. Moreover, further increase in pH causes a dual competition between negatively charged Cr(VI) species and hydroxyl ions. Predictive mathematical model indicated that the optimum process conditions were at pH 2 and at 60°C with the initial Cr(VI) concentration of 60 mg/L. Pseudo second-order model described the kinetic data very well. The positive sign of enthalpy change confirmed the endothermic nature of adsorption process. Cr(VI) adsorption mechanism was interpreted as complexation or chemisorption with the respect of high enthalpy value (54.05 kJ/mol) and fitting of pseudo second-order kinetic model.

Researchers in [30] carbonized Eichhornia crassipes root at 600°C after impregnating with concentrated H_2SO_4 at 150–165°C for 24 h. The adsorption capacity of activated carbon was 36.34 mg/g, at optimum conditions of pH 4.5 and temperature of 25°C. The experimental adsorption data were fitted to Langmuir isotherm model. Adsorption equilibrium was reached after 60 min. Pseudo second-order model is more likely to predict adsorption kinetic. The authors interpreted this result with the chemical adsorption being the rate-controlling step. The rise in Cr(VI) adsorption with the increased temperature indicated that the adsorption process is endothermic in nature. $\Delta H°$ values were 11.9 kJ/mol and 12.5 kJ/mol for different initial concentrations. Mean free adsorption energy was found to be 17.36 kJ/mol. This is due to different chemical processes accompanying the ion exchange process [30]. The maximum Cr(VI) removal capacity in column studies was 0.8 mg/g.

KOH activated carbon was developed from peanut shell [31]. During the activation process half of produced carbon was oxidized by air. The authors investigated Cr(VI) adsorption onto these unoxidized and oxidized carbons with respect of equilibrium, kinetics, and thermodynamics. BET surface area and total pore volume of oxidized and unoxidized samples are 95.51 m^2/g, 0.35 cm^3/g, and 88.85 m^2/g, 0.33 cm^3/g, respectively. Maximum adsorption capacity (about 8.4 mg/g for oxidized and 7 mg/g for unoxidized carbon) was obtained at pH 2 and a sharp decrease in the adsorption capacity occurred between pH 2 and 7, thereafter the capacity became negligible. The authors explained the high Cr(VI) adsorption with electrostatic force of attraction at low pH. It is reported that adsorption was fast in 7 h and then became slow up to 20 h, finally equilibrium occurred almost at the 24 h for both oxidized and unoxidized carbon. Chromium adsorption onto oxidized and unoxidized activated carbons followed both pseudo first-order and pseudo second-order kinetic models according to high R^2 values. However, if one can look up the experimental data and models, it is obvious that pseudo second-order model represents the results much better than the first-order one. The Cr(VI) adsorption isotherms of both carbons fitted the Langmuir model better than Freundlich model in the temperature range studied. The authors calculated enthalpy value as positive, which showed the endothermic nature of Cr(VI) adsorption. Overall, oxidized carbon had higher Cr(VI) adsorption capacity than unoxidized carbon related with high surface area, carbon content, and micropore volume of oxidized carbon.

The used biomass waste materials are tamarind wood, peanut shell, rice husk, saw dust, sugarcane bagasse, olive bagasse, almond shell, groundnut, date palm seed, sugarcane husk, eucalyptus wood, Eichhornia crassipes roots, bael fruit shell, rice straw, oil palm fiber, Trapa natans (a water chestnut), jambolanum nut, palm shell, algae bloom residue and apricot stone

in the reviewed articles. As well as the nature of precursor, activation process is also very effective on activated carbon properties. Various activation methods from physical activation like steam, CO_2, and air to chemical activation like KOH, $ZnCl_2$, H_2SO_4, and H_3PO_4 activation have been used in order to produce activated carbon. Amongst them, H_3PO_4 activation, which was the most common used, distinctively yielded with the highest surface area activated carbons. Activated carbon produced by zinc chloride activation also has high surface area. Although high surface area and high pore volume are effective for Cr(VI) adsorption, linear relationship between the high surface area and Cr(VI) adsorption capacity was not observed amongst the reviewed articles.

High surface area and pore volume are not only critical parameters but also surface chemistry of activated carbon is very important during the adsorption of charged ions like heavy metals. The possible mechanisms that could be occurred during the Cr(VI) adsorption onto activated carbon are physical adsorption, ion exchange, electrostatic attraction, chemical adsorption, and reduction to Cr(III). Surface functional groups have very important role for the all mentioned occurrences except physical adsorption by van der Waals forces. High surface functionalities may be resulted in high chromium adsorption. In case of heavy metal adsorption, surface functional groups on activated carbon surface should be defined by different analytical methods like FTIR and Boehm's titration [32]. In addition, potentiometric titration method, which was described in [33], could be used for characterizing the surface functionalities of activated carbon.

Surface functional groups can be scanned by FTIR, comprehensively, while Boehm's titration gives quantitative amount of acidic surface functionalities. The relative concentrations of acidic surface functional groups in carbons can be determined by Boehm's titration with sodium hydrogen carbonate, sodium carbonate, and sodium hydroxide [32, 34]. There are assumptions that all carboxylic, lactonic, and phenolic groups can be reacted with NaOH; Na_2CO_3 consumed by both carboxylic and lactonic groups; and $NaHCO_3$ can neutreulize only carboxylic groups.

Surface basicity of carbon is not understood yet. Delocalized π electrons on the edges of graphene sheets could be responsible for this basicity. However, it was declared in reference [34] that the basicity of these π electrons is relatively weak and some groups like quinine, diketone, chromene, and γ-pyrones on the carbon surface may cause these basic sites [35]. Titration with NaOH gives the amounts of total basic groups on carbon surface after neutralizing by HCl.

The shape of proton-binding curve, which is obtained by potentiometric titration, also indicates the presence of surface functional groups on the activated carbon surface. Carboxylic groups dissociate in the pH interval 3–6 and phenolic groups dissociate above this pH; consequently, one can say that the sharp falls of the proton binding curves on the corresponded pH range give the proton dissociations of these mentioned groups [36]. It is assumed that the anion and cation exchanges are in equilibrium at the crossover point with the pH axis on the proton binding. Carbon surface is positively charged at pH below this point, which is called point of zero charge (pH_{PZC}).

http://dx.doi.org/10.5772/60206

Cr(VI) adsorption was strongly pH-dependent. pH of the solution not only affects the Cr(VI) species but also the activated carbon surface. On raising pH, the possible reactions that occurred on the activated carbon surface are expressed as follows:

$$\text{AC-OH}_2^+ \leftrightarrow \text{AC}\left(\text{OH}\right)^0 + \text{H}^+ \quad (1)$$

$$\text{AC}\left(\text{OH}\right)^0 \leftrightarrow \text{AC-O}^- + \text{H}^+ \quad (2)$$

These surface hydroxyl groups are called protonated, neutral, and ionized, respectively. The activated carbon surface is nondissociated until pH_{PZC} and show great interest to the anions like $HCrO_4^-$ because of the electrostatic attraction, especially at low pH. After pH_{PZC} value, proton dissociation from the surface occurs; consequently, deprotonated surface repulses the anionic chromium species but attracts to the cations. Although it is very important to determine pH_{PZC} of activated carbon in order to characterize carbon surface during the pH variation, consequently affinity of carbon surface to the Cr(VI) species, only a few of the reviewed studies [17, 24] reported the pH_{PZC} of the produced activated carbon.

Overall, the following points are essentially effective on Cr(VI) adsorption onto activated carbon derived from biomass waste material:

1. Structural properties of activated carbon like surface area and pore volume
2. Surface chemistry of activated carbon [type and amount of surface functional groups, pH of point of zero charge (pH_{PZC})]
3. pH of the solution
4. Initial chromium concentration
5. Adsorbent dosage
6. Temperature
7. Contact time

These matters will be discussed in detail in the following section by using our data about Cr(VI) adsorption onto peach stone, one of the biomass waste material, based activated carbon.

3. Application of peach stone based activated carbon for Cr(VI) removal

Peach stone based activated carbon was used for Cr(VI) removal from aqueous solution. Effects of process parameters like pH, carbon dosage, contact time, and temperature on Cr(VI) adsorption will be discussed within this section. Furthermore, Cr(VI) adsorption kinetics and thermodynamics will be investigated and Cr(VI) adsorption mechanisms will be tried to illuminate.

3.1. Peach stone based activated carbon

Peach stone was converted to activated carbon by using one-step steam activation at 800°C. Detailed production conditions of peach stone based activated carbon were reported previously [37]. The some characteristics of peach stone based activated carbon are given in Table 1. N_2 adsorption measurements were performed using a Quantachrome Autosorb-1-C surface analyzer. Elemental analysis of the carbon was carried by VarioEL III CHNS elemental analyzer. The Density Functional Theory (DFT) model was applied to N_2 adsorption–desorption data to determine pore volume and pore size distribution, which is given in Figure 3.

BET surface area (m^2/g)	608
Pore volume (cm^3/g)[a]	0.341
Micropore volume (cm^3/g)[a]	0.331
Carboxylic groups (meq/g) [b]	< detection limit
Lactonic groups (meq/g) [b]	0.062
Phenolic groups (meq/g)[b]	0.254
Total Acidic groups (meq/g)[b]	0.316
Basic groups (meq/g)[b]	0.319
Point of Zero Charge (pH_{PZC})[c]	8.0
C (%)[d]	93.18
H (%)[d]	0.940
O (%)[d]	5.670
N (%)[d]	0.215

[a]Density functional theory model, [b]Boehm method, [c]obtained from potentiometric titration data, [d]elemental analysis

Table 1. Characteristics of peach stone based activated carbon [37]

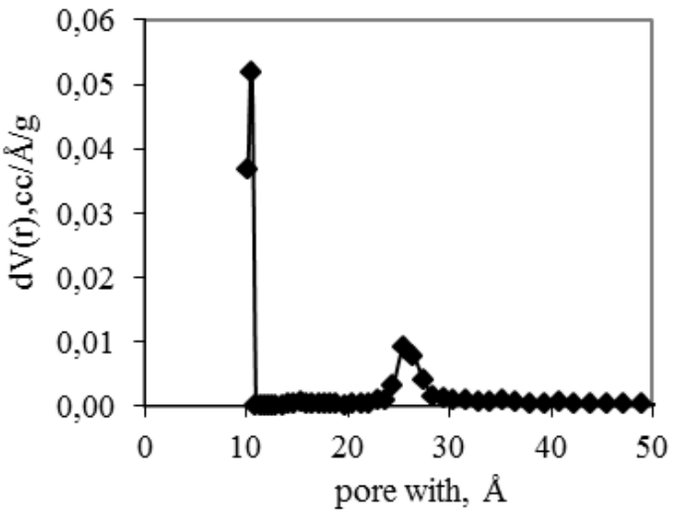


Figure 3. Pore size distribution of activated carbon

http://dx.doi.org/10.5772/60206

It is clear from Figure 3 that distribution intensity is quite high at lower than 10Å, which shows microporous structure of produced carbon. There are also an amount of pores centered between 24Å and 28Å (Figure 3). As can be seen from Table 1, approximately 97% of pore volume consists of micropores. In addition, the amounts of acidic and basic groups on activated carbon surface are almost the same.

3.2. pH effect on Cr(VI) adsorption

Experimental Cr(VI) adsorption isotherms obtained at different pH values are shown in Figure 4. All isotherm curves show typical Type 1 shape, according to IUPAC classification at pH 2, 4, and 6. Type 1 isotherms are generally given by microporous adsorbents in case of physical adsorption. Furthermore, monolayer adsorption, hence, chemical activation could be attributed for this behavior.

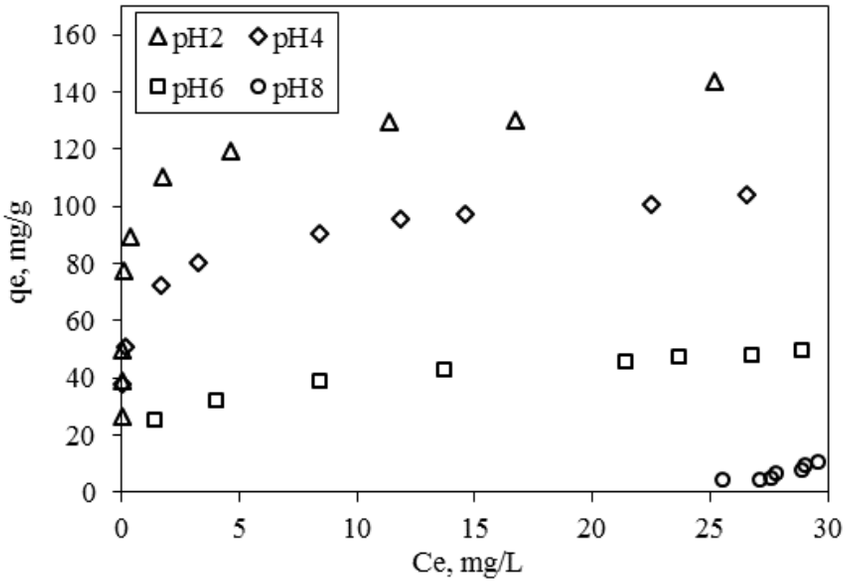


Figure 4. Experimental Cr(VI) adsorption isotherms at various pH (initial CrVI) concentration: 30 mg/L; solution volume: 50 mL; activated carbon dosage: 2–60 mg)

Cr(VI) adsorption was strongly pH-dependent and superior at low pH (Figure 4) as observed by the most researchers [14, 15, 17–19, 21–25, 27, 29, 31]. This can be evaluated by examining the adsorbate and the adsorbent surface. Cr(VI) species at different pH are shown in the following equations:

$$H_2CrO_4 \leftrightarrow H^+ + HCrO_4^- pK_a = 0.8 \quad (3)$$

$$HCrO_4^- \leftrightarrow H^+ + CrO_4^{2-} pK_a = 6.5 \quad (4)$$

$$2HCrO_4^- \leftrightarrow Cr_2O_7^{2-} + H_2O pK_a = 1.52 \quad (5)$$

All functional groups on the carbon surface are nondissociated at studied pH (2, 4, 6, 7), due to the pH_{PZC} of carbon about 8.0. These groups are protonated throughout the $[H]^+$-rich region, i.e., at low pH (Eqs. 1–2) There is an electrostatic attraction between protonated carbon surface and negatively charged hydrogen chromate ions (Eq. 3) at low pH. Maximum Cr(VI) adsorption capacity was obtained at pH 2, which was about 140 mg/g and it was decreased with increasing pH and was equal to approximately 100 mg/g, 48 mg/g, and 12 mg/g at pH 4, 6, 8, respectively (Figure 4). Activated carbon surface becomes neutral ($AC(OH)^0$) due to the proton releasing with increasing pH. Consequently, rising pH was resulted in lowering Cr(VI) adsorption capacity. Although almost all chromium was removed with 20 mg of activated carbon at pH 2, only 56% of chromium was removed at pH 6 and this value went through the 7% when studied at pH 8 (Figure 5).

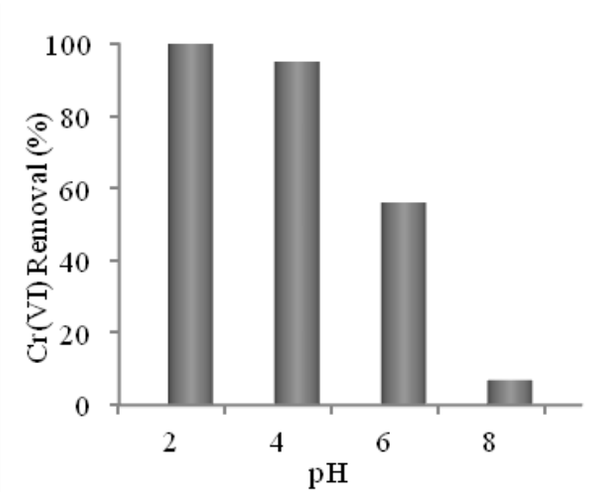


Figure 5. Cr(VI) removal percentage at different pH (initial Cr(VI) concentration: 30 mg/L; solution volume: 50 mL; activated carbon dosage: 20 mg)

As can be seen from Figure 4, chromium adsorption isotherm shapes are different and capacities are very low at studied pH 8. This can be interpreted by the competitiveness between chromate ions (CrO_4^{2-}) and hydroxyl ions; besides, one chromate ion needs two active sites because of two minus charges of it. It should also be kept in mind that proton dissociation of carbon surface starts at pH 8.0, which is the pH_{PZC} of carbon; consequently, deprotonated surface repulses the chromate anions.

3.3. Effect of pH on Cr(VI) reduction

Hydrogen chromate can reduce to Cr(III) at acidic medium [38] as demonstrated in Eqs. 6–8.

$$HCrO_4^- + \text{Organic matter} + H^+ \rightarrow Cr^{3+} + H_2O \quad (6)$$

http://dx.doi.org/10.5772/60206

$$HCrO_4^- + 7H^+ + 3e^- \rightarrow Cr^{3+} + 4H_2O \quad (7)$$

$$HCrO_4^- + 3C + H^+ \rightarrow Cr^{3+} + H_2O + 3/2\ CO_2 \quad (8)$$

Reduction of Cr(VI) was followed with the difference between the concentrations of total chromium and Cr(VI) in the solutions after treatment with activated carbon (figure was not given.). Cr(III) ions were observed only at pH 2 not at higher pH. It was also noticed that there were no big differences at low adsorbent dosages. This could be explained with low dissolved organic carbons at low adsorbent dosages. There were no differences between the total Cr and Cr(VI) concentrations at pH 4, 6, and 8. There are two possibilities: (i) there is not enough protons to reduce Cr(VI) to Cr(III) at these pH or (ii) the reduction reactions are occurred and then reduced Cr(III) ions are adsorbed on the carbon surface easily due to the low proton concentration, which compete with positively charged Cr(III) ions. Likewise, Cr(VI) could be reduced to Cr(III) in the presence of organic compounds (Eq. 6) even at neutral pH [39]. Similarly, it was suggested in [23] that Cr(VI) adsorption is mainly through a reduction to Cr(III) on activated carbon.

3.4. Effect of temperature on Cr(VI) adsorption

Increasing temperature from 22°C to 32°C caused a decrease of Cr(VI) adsorption and then capacity increased with further increment of temperature to 45°C (Figure 6). There could be several processes like ion exchange, physical adsorption, chemisorption, and reduction, which have different effects by temperature, during the Cr(VI) adsorption.

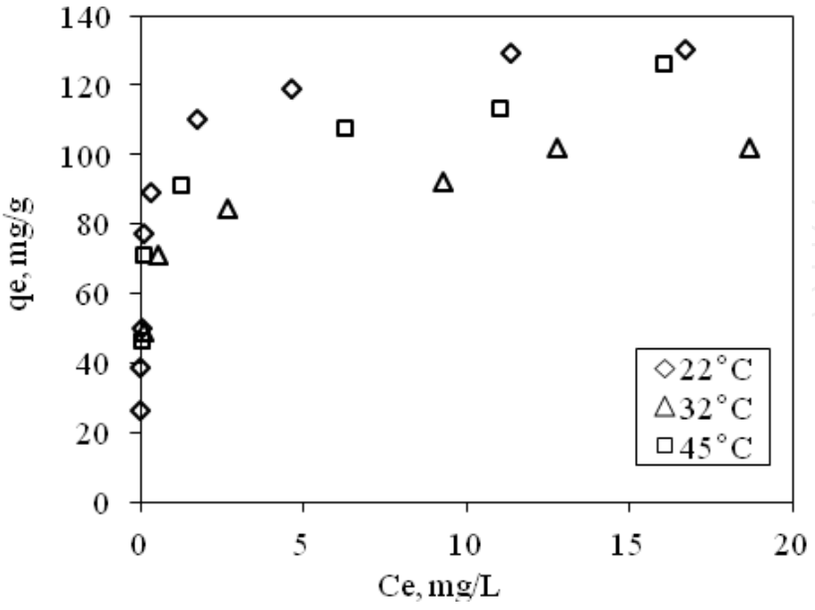


Figure 6. Experimental Cr(VI) adsorption isotherms at various temperature (initial CrVI) concentration: 30 mg/L; solution volume: 50 mL; activated carbon dosage: 2-60mg, pH:2)

It is known that ion exchange and physical adsorption capacity decreases with temperature while chemisorption and Cr(VI) reduction reaction are endothermic in nature. Cr(VI) adsorption trend by temperature could be interpreted with the combining effect of the mentioned mechanisms, that means, while ion exchange or/and physical adsorption was the predominant mechanism in the range of 22–32°C, chemisorption or/and reduction process was more effective at elevated temperature. It should also be considered that adsorption capacity could increase due to the hydrophobic effects. Elevated temperature is resulted in a decrease of hydration of $HCrO_4^-$ molecules, hence less hydrated ions could bond to the relatively hydrophobic carbon surface easily.

3.5. Effect of initial Cr(VI) concentration

Initial ion concentration is one of the process parameters that affected the adsorption capacity. Cr(VI) adsorption capacities increased with increasing initial Cr(VI) concentrations for all studied pH (Table 2).

pH		C_i: 5 mg/L	C_i: 30 mg/L	C_i: 60 mg/L
q_e, (mg/g)	2	62.9	89.1	111.7
	4	42.6	72.2	86.7
	6	19.9*	25.3	35.0

(*) obtained at 90% removal (due to could not be reached to 95% removal)

Table 2. Cr(VI) adsorption capacities at different initial Cr(VI) concentrations (capacities obtained at 95% Cr(VI) removal efficiency)

Increasing Cr(VI) adsorption capacity by initial concentration could be explained that high initial ion concentration provides an important driving force in order to overcome all mass transfer resistances between the adsorbate molecules and the adsorbent surface [40].

3.6. Adsorption isotherms

Adsorption isotherm is a unique way in order to evaluate an adsorption process as a unit operation. It not only indicates the adsorption capacity under studied conditions but also gives information about the mechanism and favorability of adsorption [41]. Langmuir and Freundlich adsorption isotherm models, which express the nonlinear relationship between the adsorbed ion on the adsorbent phase and the ion in the solution phase, are the most frequently used in the literature. These two-parameter models are simple and give a good description of experimental behavior in a large range of operating conditions [41].

The Langmuir theory, the first adsorption isotherm model developed in 1918, is on the basis of kinetic view point, and considers assumptions mentioned below:

1. Adsorption takes place in monolayer. Each active site adsorbs only one molecule.
2. There is no interaction between adsorbed molecules.
3. Adsorption enthalpy of all adsorbate molecules is equal [42].

Langmuir model is expressed by the following equation:

$$q_e = \frac{Q \cdot b \cdot C_e}{1 + b \cdot C_e} \tag{9}$$

where q_e is the amount of ions adsorbed per unit mass of adsorbent (mg/g), C_e is the equilibrium concentration of the adsorbate in the bulk solution (mg/L), Q and b are the Langmuir constants related to maximum adsorption capacity and the free energy of adsorption, respectively. Values of Q and b can be graphically determined from the linear form of the Langmuir model (Eq. 10).

$$\frac{1}{q_e} = \frac{1}{Q \cdot b \cdot C_e} + \frac{1}{Q} \tag{10}$$

Langmuir isotherm can be expressed in terms of a dimensionless separation factor, R_L, which describes the type of isotherm;

$$R_L = \frac{1}{1 + b \cdot C_0} \tag{11}$$

where C_0 is the initial concentration of Cr(VI). The magnitude of R_L determines the feasibility of adsorption process. If $R_L > 1$, adsorption is unfavorable; if $R_L = 1$, adsorption is linear; if $R_L < 1$, adsorption is favorable; and if $R_L = 0$, adsorption is irreversible [43].

The Freundlich model is one of the earliest known empirical equations based on heterogeneous surface and adsorption heat. It is expressed by the following equation:

$$q_e = K_F \cdot C_e^{1/n} \tag{12}$$

where K_F and n are indicators of adsorption capacity and adsorption intensity, respectively.

The constants k and n of the Freundlich model are respectively obtained from the intercept and the slope of the linear plot of Freundlich model (Eq. 13).

$$\ln q_e = \ln K_F + \left(1/n\right)\ln C_e \tag{13}$$

The conformity between the experimental data and the theoretical data was investigated using correlation coefficients (R^2) and error analysis. Error (%) values were calculated from Eq. 14;

$$Error(\%) = \frac{\sum_{1}^{N}\left|100 \cdot \frac{\left(q_e - q_{er}\right)}{q_e}\right|}{N} \tag{14}$$

where q_e (mg/g) and q_{et} (mg/g) are experimental and theoretical equilibrium adsorption capacities, respectively and N is the total data number.

Langmuir and Freundlich adsorption isotherm model parameters, evaluated from the linear plots, are presented in Tables 3 and 4, respectively. According to the correlation coefficients and error values, Freundlich model expressed Cr(VI) adsorption onto activated carbon better than Langmuir model.

T (°C)	*C_i (mg/L)*	**pH**	*Q (mg/g)*	*b (L/mg)*	*R^2*	**Error (%)**	*R_L*
22	5	2	100.219	14.422	0.936	8.599	0.01301
22	5	4	73.392	11.435	0.928	4.652	0.01623
22	5	6	34.978	3.109	0.917	4.851	0.05723
22	5	8	–2.371	–0.145	0.806	10.534	4.22181
22	30	2	112.167	97.453	0.843	13.880	0.00033
22	30	4	89.106	17.331	0.862	10.233	0.00183
22	30	6	47.960	0.743	0.939	5.067	0.04079
22	30	8	–1.041	–0.031	0.885	9.473	36.3553
22	60	2	123.436	84.386	0.865	14.781	0.00019
22	60	4	99.618	9.599	0.908	7.459	0.00163
22	60	6	53.373	35.983	0.759	16.076	0.00046
22	60	8	–2.624	–0.014	0.878	7.393	8.00448
32	30	2	92.302	13.705	0.926	7.110	0.00254
45	30	2	101.079	103.184	0.883	12.512	0.00034

Table 3. Langmuir adsorption isotherm constants

http://dx.doi.org/10.5772/60206

T (°C)	C_i (mg/L)	pH	K_F (mg/g)	*n*	R^2	Error (%)
22	5	2	89.203	4.566	0.981	3.277
22	5	4	61.780	6.024	0.992	1.371
22	5	6	24.302	4.386	0.991	1.722
22	5	8	0.022	0.283	0.736	11.609
22	30	2	97.597	8.122	0.979	4.160
22	30	4	65.655	6.793	0.986	2.997
22	30	6	23.772	4.578	0.995	1.159
22	30	8	$6.14.10^{-11}$	0.131	0.884	11.982
22	60	2	105.026	8.849	0.942	7.247
22	60	4	60.663	5.814	0.964	9.886
22	60	6	37.629	7.874	0.951	5.859
22	60	8	$1.52.10^{-7}$	0.224	0.899	8.817
32	30	2	71.769	7.675	0.970	4.086
45	30	2	88.146	8.288	0.979	4.005

Table 4. Freundlich adsorption isotherm constants

Although a significant amount of researchers [17, 19, 24–26] indicated the same result, there are also many workers [15, 30, 31] who reported that Cr(VI) adsorption onto activated carbon fitted the Langmuir model. Furthermore, there are some studies [18, 21, 22, 27] which reported that both Freundlich and Langmuir models described Cr(VI) adsorption onto activated carbon very well.

Dimensionless separation factors, R_L, show that the adsorption onto activated carbon is favorable except pH 8 (Table 3). Furthermore, calculated R_L values are very close to the zero for pH 2 and 4, which indicates the irreversible Cr(VI) adsorption, and consequently quite strong interaction between hydrogen chromate anions and activated carbon surface.

3.7. Adsorption kinetics

The rate at which dissolved heavy metal ions are removed from aqueous solution by solid adsorbents is a significant factor for application in water quality control. The rapid adsorption processes are quite useful for practical use, due to the need of short contact time in the actual process. When stoichiometric amount of activated carbon dosage (0.4 g/L) was used, more than 24 h (not shown in figure) were required in order to remove all chromium (Figure 7). However, almost all Cr(VI) was adsorbed within 1.5 h for the case of twice of stoichiometric carbon dosage.

There are different equilibrium times from 60 min to 24 h for Cr(VI) adsorption onto activated carbon in the literature [15, 18, 22, 25, 27, 29–31]. However, all of the given results did not reflect

the same conditions as used in this study; it can be concluded that 1.5 h equilibrium time is applicable.

It is essential to evaluate adsorption kinetics as well as adsorption equilibrium using theoretical models in order to design and control the adsorption process units. Pseudo first-order and pseudo second-order kinetic models were used to perform the Cr(VI) adsorption kinetics. Both models include all steps of adsorption such as external film diffusion, adsorption, and internal particle diffusion, so they are pseudo models [41].

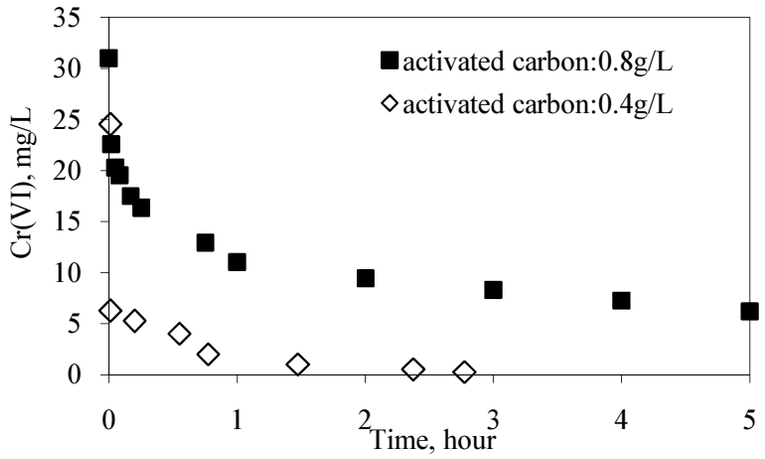


Figure 7. Effect of contact time on Cr(VI) adsorption

The *pseudo first-order kinetic model* can be expressed as follows:

$$\frac{\mathrm{d}q_t}{\mathrm{d}t} = k_1 \cdot \left(q_e - q_t\right) \tag{15}$$

where k_1 is the rate constant of pseudo first-order model (per min) and q_e and q_t denote the adsorption capacity at equilibrium and at time t (mg/g), respectively.

After integration of Eq. 15 by applying boundary conditions, $q_t = 0$ at $t = 0$ and $q_t = q_t$ at $t = t$, becomes

$$\log\left(\frac{q_e}{q_e - q_t}\right) = \frac{k_1 \cdot t}{2.303} \tag{16}$$

A plot of log ($q_{eq} - q_t$) against t should give a straight line to confirm favorability of kinetic model. The plot of log ($q_{eq} - q_t$) against t did not give any straight line (R^2 =0.731–0.900) for all kinetic data; consequently, it was concluded that the Cr(VI) adsorption kinetics did not fit the pseudo first-order equation.

http://dx.doi.org/10.5772/60206

The *pseudo second-order kinetic model* suggests that adsorption process involves chemisorption mechanism [41] and can be expressed as follows:

$$\frac{dq_t}{dt} = k_2 \cdot \left(q_e - q_t\right)^2 \tag{17}$$

where k_2 is the rate constant of second-order model. For the same boundary conditions, the integrated form of Eq. 17 becomes

$$\frac{t}{q_t} = \frac{1}{k_2 \cdot q_e^2} + \frac{1}{q_e} \cdot t \tag{18}$$

If the experimental data fit the second-order kinetics, the plot of t/q against t should give linear relationship. q_e and k_2 can be determined from the slope and intercept of this plot. Initial adsorption rates (h, mg/g, min) were also calculated from the data of pseudo second-order kinetic model according to the Eq. (19) [44]:

$$h = k_2 . q_e^{\ 2} \tag{19}$$

Pseudo second-order kinetic model expressed the Cr(VI) adsorption kinetics very well at all the studied conditions (Table 5).

T (°C)	AC (g/L)	C_i (mg/L)	q_e exp (mg/g)	q_e calc (mg/g)	k_2 (g/mg.h)	h, init. rate* (mg/g.min)	R^2
22	0.4	30	72.93	73.10	0.0290	2.584	0.997
22	0.8	30	33.56	33.57	0.8464	15.894	0.999
32	0.4	30	67.52	67.96	0.0304	2.339	0.998
45	0.4	30	69.56	70.09	0.0319	2.615	0.998

Table 5. Pseudo second-order kinetic model parameters

This situation can be followed with extremely high correlation coefficients ($R^2 = 0.997 – 0.999$). Moreover, there is an excellent correlation between calculated q_e values and experimental q_e values. As can be known that pseudo second-order kinetic model involves chemisorption mechanism, hence it can be suggested that Cr(VI) adsorption onto prepared activated carbon is based on chemical adsorption. Similarly, almost all researchers expressed their kinetic data by using pseudo second-order kinetic model [15, 18, 19, 21, 22, 24, 25, 27, 31]. The rate constant and the initial rate increased with temperature, as expected (Table 5). It is interesting when activated carbon dosage was increased two times, Cr(VI) adsorption rate constant increased

about 30 times. Diffusion is an endothermic process; an increase in temperature causes a raise on the diffusion rate of the adsorbate molecules across the external boundary layer and within the pores.

3.8. Regeneration of activated carbon

Regeneration studies were carried out by using different concentrations of acid, alkali, and salt solutions during the five cycles of adsorption–desorption studies. The best regeneration was obtained with 10% NaOH and 10% HCl solutions (Figure 8).

Although it is typical to use salt (NaCl) and caustic-salt (NaOH.NaCl) for chromate recovery from anion exchangers in the treatment of cooling water [45], these solutions were not effective for regeneration of peach stone activated carbon. Although regeneration percentages increased across the cycles, Cr(VI) adsorption capacity decreased about 55% of initial value (Figure 9).

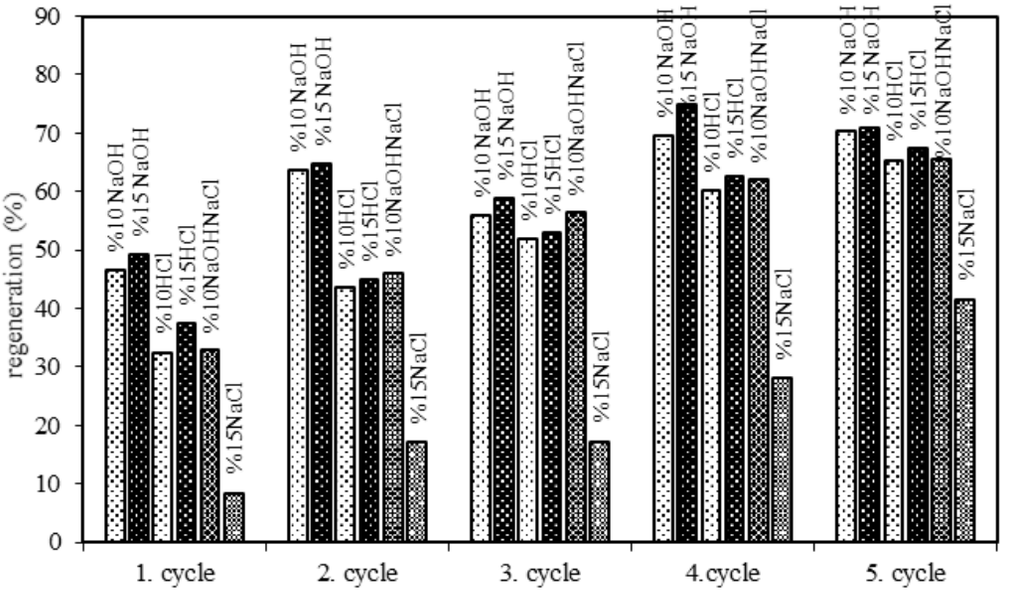


Figure 8. Regeneration percentages during the adsorption–desorption cycles

It can be concluded that Cr(VI) adsorption capacity of activated carbon is considerably high, but regeneration of it is not good. Similarly, irreversible Cr(VI) adsorption onto nitric acid oxidized activated carbon has been indicated in reference [46]. Many researchers reported the regeneration problems of Cr(VI) exhausted activated carbons [3, 19, 24].

3.9. Activation energy

The activation energy, E_A, was determined using the Arrhenius equation

$$k_{ad} = k_0 . e^{\frac{-E_A}{R.T}} \tag{20}$$

http://dx.doi.org/10.5772/60206

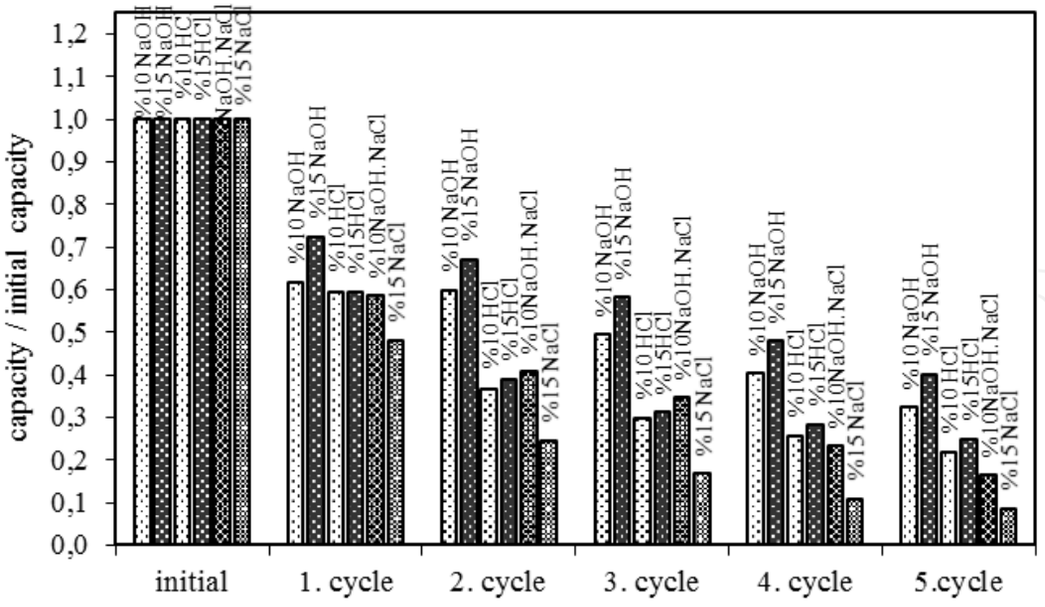


Figure 9. Cr(VI) adsorption capacity variations during the adsorption–desorption cycles

where k_{ad} is the adsorption rate, k_0 is the pre-exponential factor, and R is the gas constant. Linear form of Eq. 20 can be written as in below:

$$\ln k_{ad} = \ln k_0 - \frac{E_A}{R.T} \tag{21}$$

The plot of ln k_{ad} against to $1/T$ was found linear ($R^2 = 0.9991$). The activation energy, E_A, was calculated from the slope as 3.249 kJ/mol.

Because the energy requirement of physical adsorption is very low, activation energy of physical adsorption is usually not more than 4.184 kJ/mol [47]. Although activation energy of chromium adsorption onto peach stone based activated carbon is very low and could be a sign of physical adsorption, irreversible chromium adsorption process gets into mind the chemical interaction; consequently, activation energy is expected to be higher than 4.184 kJ/mol. Two kinds of chemisorption: activated and, less frequently, nonactivated have been defined in reference [47]. Reaction rate varies with the temperature on the base of Arrhenius equation (high E) in case of activated chemisorption. For nonactivated chemisorption, reaction occurs extremely fast, suggesting the activation energy is near zero [48]. Actually, reaction rate constant of chemisorption increases with temperature so the activation energy can be calculated relatively high. On the other hand, if the diffusion to the pores is very low, apparent rate may not be show a significant raise by temperature. Consequently, apparent activation energy can be calculated from the slope of the plot between 1/T and ln K as relatively low [49]. It can be concluded that, activation energy of chromium adsorption onto activated carbon was calculated very low, because of the diffusion resistance of pores. In addition, relatively low activation energy suggested that Cr(VI) adsorption was a diffusion controlled process [48].

3.10. Mean free sorption energy, *E*

The mean free sorption energy, *E*, is defined as free energy change when one mole of adsorbate in aqueous phase is transferred to the solid surface.

It is calculated by the following equation [44]:

$$E = \frac{1}{\left(2\beta\right)^{1/2}} \tag{22}$$

β is the constant related to the sorption energy (mol^2/kJ^2) and could be calculated by using Dubinin–Radushkevich (D–R) equation. Linearized D-R equation can be written as follows:

$$\ln q_e = \ln q_m - \beta \cdot \varepsilon^2 \tag{23}$$

where q_e and q_m are equilibrium and maximum adsorption capacity (mol/g), respectively, ε is the Polanyi potential. In order to obtain Polanyi potentials, experimental adsorption data should be applied to Eq. (24).

$$\varepsilon = R \cdot T \cdot \ln\left(1 + \frac{1}{C_e}\right) \tag{24}$$

A linear plot of ln q_e against ε^2 gives the values of β and q_m. Thus the mean free energy of adsorption, E, can be calculated by using Eq. (22).

The mean free sorption energy for ion exchange processes is between 8 and 16 kJ/mol, and activation energy of physical adsorption is not higher than 4.184 kJ/mol [47]. In this study, mean free sorption energy values were calculated >22 kJ/mol at pH 2 (Table 6), which indicates chemical interaction between carbon surface and hydrogen chromate ions. This chemical interaction could consist of reduction reactions of Cr(VI).

pH	*T (°C)*	*E (kJ/mol)*	R^2
2	22	23.63	0.995
2	32	22.81	0.985
2	45	26.12	0.987
4	22	20.98	0.993
6	22	15.68	0.998
8	22	2.10	0.956

Table 6. Mean free adsorption energy of Cr(VI) adsorption (C_i:30 mg/L)

3.11. Adsorption thermodynamics

Thermodynamic parameters such as Gibbs free energy ($\Delta G°$), enthalpy ($\Delta H°$), and entropy ($\Delta S°$) changes can be determined from the variation of thermodynamic equilibrium constant, K, at different temperatures. K values were determined by using the following equation:

$$K = \frac{C_{Ae}}{C_e} \tag{25}$$

where C_{Ae} (mg/g) and C_e (mg/g) indicate the Cr(VI) amounts on adsorbent phase and solution phase, respectively. The standard enthalpy change of adsorption ($\Delta H°$) and the standard entropy change of adsorption ($\Delta S°$) could be calculated from the slope and intercept of Van't Hoff plot (ln K versus 1/T), respectively.

$$\ln K = -\frac{\Delta H°}{RT} + \frac{\Delta S°}{R} \tag{26}$$

R (8.314 kJ/(mol.K)) refers to the universal gas constant and T (K) denotes the absolute temperature. The standard free energy changes of adsorption ($\Delta G°$) is determined according to Eq. (27).

$$\Delta G° = -R.T.\ln K \tag{27}$$

T (°C)	*K (10^5)*	ΔG° (kJ/mol)
22	4.022	-31.650
32	0.348	-26.515
45	1.787	-31.973

Table 7. Thermodynamic parameters of Cr(VI) adsorption (at pH 2; C_i:30 mg/L)

Thermodynamic data obtained for 30 mg/L initial Cr(VI) concentration at pH 2 were given in Table 7. The Gibbs free energy change values were found as negative, which indicated the feasibility and spontaneity of the adsorption.

3.12. Cr(VI) adsorption mechanism

Investigation with X-ray photoelectron spectroscopy (XPS) could provide valuable information in order to examine adsorption mechanism. Elemental analysis of carbon, oxygen, and other elements can be done by using XPS technique. In addition, by determining the shift in binding energies, XPS analysis provides valuable information about the chemical state of adsorbed ions onto activated carbon [50].

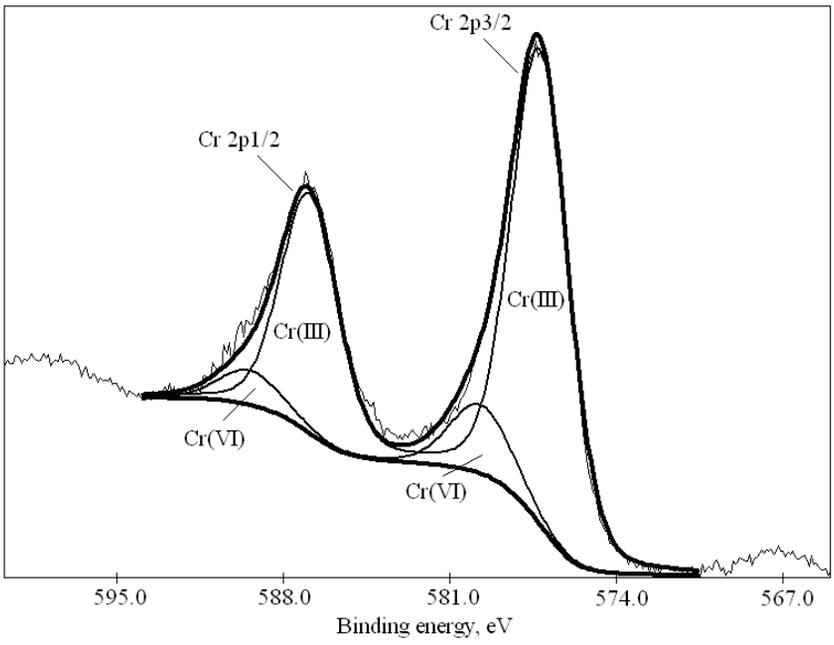


Figure 10. XPS spectrum(Cr $2p^{1/2}$ and Cr $2p^{3/2}$ orbitals) of Cr(VI) exhausted activated carbon (at pH 2 and C_i:30 mg/L)

According to the XPS results corresponding $Cr2p^{1/2}$ and $Cr2p^{3/2}$ orbitals, there are two separate bands for both orbitals (Figure 10). Significant bands appeared at binding energies of 577.0–578.0 eV for Cr2p3/2 and at binding energies of 586.0–588.0 eV for Cr2p1/2 orbital. They correspond to trivalent chromium. CrO_3 was characterized by higher binding energies; 580.0–580.5 eV and 589.0–590.0 eV, since the hexavalent form draws electrons more strongly than the trivalent form [51].

XPS showed that 86% of adsorbed chromium is in Cr(III) form. In other words, some of Cr(VI) adsorbed directly while a significant amount of Cr(VI) adsorbed to the surface after reducing the trivalent form during the adsorption process. Although original carbon surface is not suitable to adsorb cations, carbon surface is oxidized as a result of reduction reaction, and oxidized carbon surface is more attractive for Cr(III) cations than the former situation. Nevertheless, a little amount of Cr(III) was released into the aqueous phase due to electrostatic repulsion between the positively charged groups and Cr(III) ions at pH 2.

4. Conclusion

Adsorption of Cr(VI) onto activated carbon derived from different biomass waste materials, have been reviewed and the factors that influenced the Cr(VI) adsorption were discussed by using both literature and experimental data. Peach stone, one of the biomass waste materials, was used as an activated carbon precursor. Prepared activated carbons showed high Cr(VI) adsorption capacity. Cr(VI) adsorption was strongly pH-dependent and superior at low pH. Freundlich model well expressed Cr(VI) adsorption. Adsorption kinetics followed the pseudo second-order kinetic model which consists of chemisorption.

Low activation energy was interpreted with nonactivated chemisorption. High mean free sorption energy was assigned with chemical interaction between carbon surface and hydrogen chromate. XPS results showed that 86% of adsorbed chromium is in its trivalent form. Possible adsorption mechanism was suggested in three steps: (i) Cr(VI) adsorption onto positively charged groups, (ii) reduction to Cr(III), (iii) adsorption of Cr(III) while a little amount of it released to the aqueous phase. Peach stone based activated carbon could be evaluated as a potential adsorbent to remove Cr(VI) from aqueous media effectively.

Author details

Dilek Duranoğlu* and Ulker Beker

*Address all correspondence to: dduran@yildiz.edu.tr

Chemical Engineering Department, Yıldız Technical University, Istanbul, Turkey

References

[1] EPA. In situ treatment of soil and groundwater contaminated with chromium. Technical Report:EPA/625/R-00/005. Washington; 2000.

[2] Weiner ER. Applications of Environmental Chemistry, A Practical Guide For Environmental Professionals. Florida: CRC Press; 2000.

[3] Mohan D, Pittman U. Activated carbons and low cost adsorbents for remediation of tri- and hexavalent chromium from water. J Hazard Mater 2006;B137:762–811.

[4] Irwin RJ. Environmental Contaminants Encyclopedia chromium VI (Hexavalent Chromium) Entry. National Park Service Water Resources Divisions. Colorado; 1997.

[5] Kozlowski CA, Walkowiak W. Removal of chromium(VI) from aqueous solutions by polymer inclusion membranes. Water Res 2002;36:4870–76.

[6] Lazaridis NK, Bakoyannakis DN, Deliyanni EA. chromium(VI) sorptive removal from aqueous solutions by nanocrystalline akaganeite. Chemosphere 2005;58:, 65–73.

[7] Khezami L, Capart R. Removal of chromium(VI) from aqueous solution by activated carbons: kinetic and equilibrium studies. J Hazard Mater 2005;B123:223–31.

[8] Hu J, Lo IMC, Chen G. Comparative study of various magnetic nanoparticles for Cr(VI) removal. Sep Purif Tech 2007;56:249-56.

[9] Anirudhan TS, Jalajamony S, Suchithra PS. Improved performance of a cellulose-based anion exchanger with tertiary amine functionality for the adsorption of chro-

mium(VI) from aqueous solutions. Coll Surf A: Physicochem Eng Asp 2009;335:107–13.

[10] Lalvani SB, Wiltowski T, Hübner AH, Weston A, Mandich N. Removal of hexavalent chromium and metal cations by a selective and novel carbon adsorbent. Carbon 1998;36:1219–26.

[11] Kobya M. Removal of Cr(VI) from aqueous solutions by adsorption onto hazelnut shell activated carbon: kinetic and equilibrium studies. Bioresour Technol 2004;91:317–21.

[12] Sulaymon AH, Abid BA, Al-Najar JA. Removal of lead copper chromium and cobalt ions onto granular activated carbon in batch and fixed-bed adsorbers. Chem Eng J 2009;155:647–53.

[13] Gosh PK. Hexavalent chromium [Cr(VI)] removal by acid modified waste activated carbons. J Hazard Mater 2009;171:116–22.

[14] Dubey SP, Gopal K. Adsorption of chromium(VI) on low cost adsorbents derived from agricultural waste material: a comparative study. J Hazard Mater 2007;145:465–70.

[15] Demiral H, Demiral I, Tümsek F, Karabacakoglu B. Adsorption of chromium(VI) from aqueous solution by activated carbon derived from olive bagasse and applicability of different adsorption models. Chem Eng J 2008;144:188–96.

[16] Duranoglu D, Trochimczuk AW, Beker U. Kinetics and thermodynamics of hexavalent chromium adsorption onto activated carbon derived from acrylonitrile-divinylbenzene copolymer. Chem Eng J, 2012;187:193–202.

[17] Demirbas E, Kobya M, Konukman AES. Error analysis of equilibrium studies for the almond shell activated carbon adsorption of Cr(VI) from aqueous solutions. J Hazard Mater 2008;154:787–94.

[18] El Nemr A, Khaled A, Abdelwahab O, El-Sikaily A. Treatment of wastewater containing toxic chromium using new activated carbon developed from date palm seed. J Hazard Mater 2008;152:263–75.

[19] Isa MH, Ibrahim N, Aziz HA, Adlan MN, Sabiani NHM, Zinatizadeh AAL, Kutty SRM. Removal of chromium(VI) from aqueous solution using treated oil palm fibre. J Hazard Mater 2008;152:662–68.

[20] Giraldo-Gutiérrez L, Moreno-Piraján JC. Pb(II) and Cr(VI) adsorption from aqueous solution on activated carbons obtained from sugar cane husk and sawdust. J Anal Appl Pyrolysis 2008;81:278–84.

[21] Acharya J, Sahu JN, Sahoo BK, Mohanty CR, Meikap BC. Removal of chromium(VI) from wastewater by activated carbon developed from tamarind wood activated with zinc chloride. Chem Eng J 2009;150:25–39.

[22] Bansal M, Singh D, Garg VK. A comparative study for the removal of hexavalent chromium from aqueous solution by agriculture wastes carbons. J Hazard Mater 2009;171:83–92.

[23] Hsu NH, Wang SL, Liao YH, Huang ST, Tzou YM, Huang YM. Removal of hexavalent chromium from acidic aqueous solutions using rice straw-derived carbon. J Hazard Mater 2009;171:1066–70.

[24] Liu W, Zhang J, Zhang C, Wang Y, Li Y. Adsorptive removal of Cr(VI) by Fe-modified activated carbon prepared from Trapa natans husk. Chem Eng J 2010;162:677–84.

[25] Muthukumaran K, Beulah S. Removal of chromium(VI) from wastewater using chemically activated Syzygium jambolanum nut carbon by batch studies. Proc Environ Sci 2010;4:266–80.

[26] Owlad M, Aroua MK, Daud WMAW. Hexavalent chromium adsorption on impregnated palm shell activated carbon with polyethyleneimine. Bioresour Technol 2010;01:5098–103.

[27] Zhang H, Tang Y, Cai D, Liu X, Wang X, Huang Q, Yu Z. Hexavalent chromium removal from aqueous solution by algal bloom residue derived activated carbon: equilibrium and kinetic studies. J Hazard Mater 2010;181:801–08.

[28] Cronje KJ, Chetty K, Carsky M, Sahu JN, Meikap BC. Optimization of chromium(VI) sorption potential using developed activated carbon from sugarcane bagasse with chemical activation by zinc chloride. Desalination 2011;275:276–84.

[29] Özdemir E, Duranoğlu D, Beker Ü, Avcı AÖ. Process optimization for Cr(VI) adsorption onto activated carbons by experimental design. Chem Eng J 2011;172:207– 18.

[30] Giri AK, Patel R, Mandal S. Removal of Cr(VI) from aqueous solution by Eichhornia crassipes root biomass-derived activated carbon. Chem Eng J, 2012;185–186:71–81.

[31] AL-Othman ZA, Ali R, Naushad M. Hexavalent chromium removal from aqueous medium by activated carbon prepared from peanut shell: adsorption kinetics, equilibrium and thermodynamic studies. Chem Eng J 2012;184:238–47.

[32] Boehm HP. Advances in Catalyst. New York: Academic Press; 1966.

[33] Helfferich F. Ion Exchange. New York: Dover Publications; 1995.

[34] Boehm HP. Surface oxides on carbon and their analysis: a critical assessment. Carbon 2002;40:145–49.

[35] Marsh H, Rodriguez-Reinoso F. Activated Carbon. Oxford: Elsevier Science & Technology Books; 2006.

[36] Strelko V Jr, Malik DJ, Streat M. Characterization of the surface of oxidized carbon adsorbents. Carbon 2002;40:95–104.

[37] Duranoglu D, Trochimczuk AW, Beker U. A comparison study of peach stone and acrylonitrile-divinylbenzene copolymer based activated carbons as chromium(VI) sorbents. Chem Eng J, 2012;165:56–63.

[38] Selomulya C, Meeyoo V, Amal R. Mechanisms of Cr(VI) removal from water by various types of activated carbons. J Chem Technol Biotechnol 1999;74:111–22.

[39] Tsuruhara T, Takehara K, Yoshimura K, Matsuoka S, Saputro S, Aizawa J. Kinetic study on Cr(VI) reduction in natural water by means of flow injection-solid phase spectrometry (FI-SPS): Proc 4th Int Conf Ion Exchange, 15–19 October 2007, Chiba, Japan.

[40] Malkoc E, Nuhoglu Y. Potential of tea factory waste for chromium(VI) removal from aqueous solutions: thermodynamic and kinetic studies. Sep Purif Technol 2007;54:291–8.

[41] Aksu Z, Balibek E. Chromium(VI) biosorption by dried Rhizopus arrhizus: effect of salt (NaCl) concentration on equilibrium and kinetic parameters. J Hazard Mater 2007;145:210–20.

[42] Woodard F. Industrial Waste Treatment Handbook. USA: Butterworth-Heinemann; 2001.

[43] Hall KR, Eagletow LC, Acrivos A, Vermeulen T. Pore and solid kinetics in fixed-bed adsorption under constant-pattern condition. Ind Eng Chem Fund 1966;5:212–23.

[44] El-Kamash AM, Zaki AA, Abed El Geleel M. Modeling batch kinetics and thermodynamics of zinc and cadmium ions removal from waste solutions using synthetic zeolite A. J Hazard Mater 2005;B127:211–20.

[45] Letterman RD. Water Quality and Treatment. New York: McGraw-Hill; 1999.

[46] Dobrowolski R, Otto M. Study of chromium(VI) adsorption onto modified activated carbons with respect to analytical application. Adsorption 2010;16:279–86.

[47] Sag Y, Kutsal T. Determination of the biosorption activation energies of heavy metal ions on Zoogloea ramigera and Rhizopus arrhizus. Process Biochem 2000;35:801–07.

[48] Raji C, Anirudhan ST. Batch Cr(VI) removal by polyacrylamide-grafted sawdust: kinetics and thermodynamics. Water Res 1998;32(12):3772–80.

[49] Levenspiel O. Chemical Reactor Omnibook. Oregon: OSU Book Store; 1989.

[50] Zhao N, Wei N, Li J, Qiao Z, Cui J, He F. Surface properties of chemically modified activated carbons for adsorption rate of Cr(VI). Chem Eng J 2005;115:133–38.

[51] Park D, Yun YS, Park JM. XAS and XPS studies on chromium-binding groups of biomaterial during Cr(VI) biosorption. J Colloid Interface Sci 2008;317:54–61.